DENNE, W. A. (1977). *Acta Cryst.* A33, 438–440.

DUNITZ, J. D. (1979). *X-ray Analysis and the Structure of Organic Molecules.* Ithaca, New York: Cornell University Press.

EISENSTEIN, M. (1979). *Acta Cryst.* B35, 2614–2625.

ELLISON, R. D., JOHNSON, C. K. & LEVY, H. A. (1971). *Acta Cryst.* B27, 333–344.

ERIKSSON, A. & HERMANSSON, K. (1983). *Acta Cryst.* B39, 703–711.

HARADA, J. & SAKATA, M. (1974). *Acta Cryst.* A30, 77–82.

HARKEMA, S., DAM, J., VAN HUMMEL, G. J. & REUVERS, A. J. (1980). *Acta Cryst.* A35, 616–621.

HIRSHFELD, F. L. & HOPE, H. (1980). *Acta Cryst.* B36, 406–415.

ISHII, M. & SCHERINGER, C. (1979). *Acta Cryst.* A35, 613–616.

JEFFREY, G. A., RUBLE, J. R., MCMULLAN, R. K., DEFREES, D. J., BINKLEY, J. S. & POPLE, J. A. (1980). *Acta Cryst.* B36, 2292–2299.

JEFFREY, G. A., RUBLE, J. R., MCMULLAN, R. K., DEFREES, D. J. & POPLE, J. A. (1981*a*). *Acta Cryst.* B37, 1381–1387.

JEFFREY, G. A., RUBLE, J. R., MCMULLAN, R. K., DEFREES, D. J. & POPLE, J. A. (1981*b*). *Acta Cryst.* B37, 1885–1890.

JEFFREY, G. A., RUBLE, J. R., MCMULLAN, R. K., DEFREES, D. J. & POPLE, J. A. (1982). *Acta Cryst.* B38, 1508–1513.

JEFFREY, G. A., RUBLE, J. R. & POPLE, J. A. (1982). *Acta Cryst.* B38, 1975–1980.

JEFFREY, G. A., RUBLE, J. R. & YATES, J. H. (1983). *Acta Cryst.* B39, 388–394.

JOHNSON, C. K. (1970). In *Thermal Neutron Diffraction*, edited by B. T. M. WILLIS, pp. 132–160. New York: Oxford Univ. Press.

KLOOSTER, W. T., SWAMINATHAN, S., NANNI, R. & CRAVEN, B. M. (1992). *Acta Cryst.* B48, 217–227.

LE PAGE, Y. & GABE, E. J. (1979). *Acta Cryst.* A35, 73–78.

SAKATA, M. & HARADA, J. (1976). *Acta Cryst.* A32, 426–433.

SWAMINATHAN, S., CRAVEN, B. M. & MCMULLAN, R. K. (1985). *Acta Cryst.* B41, 113–122.

WILLIS, B. T. M. & PRYOR, A. W. (1975). *Thermal Vibrations in Crystallography*, pp. 233–242. London: Cambridge Univ. Press.

Molecular Conformations and Crystal Packing Properties of Five 4-Alkyl-*N*-(4-cyanophenyl)piperidines by X-ray Diffraction: a Surprising Dependence upon Alkyl Chain Length

BY BASHIR M. SHEIKH-ALI, MIROSLAV RAPTA, GEOFFREY B. JAMESON AND RICHARD G. WEISS

Department of Chemistry, Georgetown University, Washington, DC 20057, USA

Abstract

The molecular structure and crystal packing of a homologous series of 4-*n*-alkyl-*N*-(4-cyanophenyl)piperidines (I), where alkyl equals butyl, pentyl, hexyl, heptyl and octyl ($n = 4$–8), have been analyzed. Although the conformations of the (cyanophenyl)piperidyl unit remain fairly constant throughout, the crystal packing depends acutely upon alkyl chain length with one, two or four molecules comprising the asymmetric unit: for (I) ($n = 4$), monoclinic ($P2_1$); for (I) ($n = 5$), monoclinic ($P2_1/c$); for (I) ($n = 6$), triclinic ($P\bar{1}$); for (I) ($n = 7$), triclinic ($P\bar{1}$); for (I) ($n = 8$), monoclinic ($P2_1/c$). The piperidyl rings are in a chair conformation. Unit-cell and other crystal data are presented.

Introduction

It is known that *trans*-1-*n*-alkyl-4-(4-cyanophenyl)cyclohexanes form monotropic smectic and enantiotropic nematic mesophases between the temperatures of the crystal and liquid phases (Eidenschink, Erdman, Krause & Pohl, 1977). To determine the influence of the isoelectronic substitution of C—H by nitrogen at the juncture between the phenyl and cyclohexyl rings, we have synthesized a series of 4-*n*-alkyl-*N*-(4-cyano-

phenyl)piperidines, (I) ($n = 4$–8). Surprisingly, only (I) ($n = 6$) is mesogenic and becomes (monotropic) nematic when cooled from the liquid state. In other work, we have shown that mesomorphism can be induced by mixing homologues of (I) (Sheikh-Ali & Weiss, 1991, 1994). In order to explore possible links between the lack of liquid crystallinity in (I) and modes of packing in the solid state, the crystal structures have been analyzed and compared with each other and with their cyclohexyl analogues.

Experimental

Table 1 lists the experimental conditions and the final refinement parameters for (I) ($n = 4$–8). Samples of (I) (Sheikh-Ali & Weiss 1991, 1994) were recrystallized from hexane and affixed to a glass fiber by epoxy resin (sans hardener). Data were collected on a Siemens P4/RA diffractometer with an LT-2 low-temperature device. No phase transitions were detected by differential scanning calorimetry between room temperature and 203 K. The phase problem was solved, in some cases with difficulty, by standard direct methods, or integrated Patterson search methods (PATSEE; Sheldrick, 1985). The structures were developed by difference-Fourier calculations interspersed with cycles of full-matrix least-

Table 1. *Crystal data and structure refinement parameters for* (I) ($n = 4$–8)

	(I) ($n = 4$)	(I) ($n = 5$)	(I) ($n = 6$)	(I) ($n = 7$)	(I) ($n = 8$)
Empirical formula	$C_{16}H_{22}N_2$	$C_{17}H_{24}N_2$	$C_{18}H_{26}N_2$	$C_{19}H_{28}N_2$	$C_{20}H_{30}N_2$
Formula weight	242.40	256.43	270.41	284.49	298.46
Temperature (K)	203	203	203	173	203
Radiation	Mo $K\alpha$	Mo $K\alpha$	Mo $K\alpha$	Mo $K\alpha$	Cu $K\alpha$
Wavelength (Å)	0.71073	0.71073	0.71073	0.71073	1.54178
Crystal system	Monoclinic	Monoclinic	Triclinic	Triclinic	Monoclinic
Space group	$P2_1$	$P2_1/c$	$P\bar{1}$	$P\bar{1}$	$P2_1/c$
Unit-cell dimensions					
a (Å)	8.317 (2)	9.065 (2)	6.369 (3)	11.061 (1)	12.331 (2)
b (Å)	17.435 (3)	9.750 (2)	9.071 (3)	15.690 (3)	11.086 (2)
c (Å)	20.011 (4)	35.191 (7)	14.682 (4)	21.641 (3)	13.929 (3)
α (°)			106.69 (2)	106.06 (1)	
β (°)	90.43 (3)	97.10 (3)	93.69 (3)	101.27 (1)	102.74 (3)
γ (°)			93.33 (3)	100.13 (1)	
Volume (Å³)	2901.7 (10)	3086.5 (11)	808.2 (5)	3432.6 (9)	1857.2 (6)
No. of reflections	34	38	36	60	26
θ range (°)	10–25	10–25	10–25	10–25	10–25
Z	8	8	2	8	4
D_x (g cm⁻³)	1.110	1.103	1.111	1.101	1.067
Absorption coefficient (mm⁻¹)	0.065	0.060	0.065	0.060	0.438
$F(000)$	1056	1120	296	1248	656
Crystal size (mm)	0.4 × 0.3 × 0.3	0.4 × 0.3 × 0.3	0.4 × 0.3 × 0.3	0.5 × 0.3 × 0.3	0.4 × 0.3 × 0.2
θ range for data collection (°)	1.55–24.99	2.26–25.00	2.35–28.64	1.94–25.00	5.15–48.72
Index range h	$-1 \to 9$	$-10 \to 10$	$-1 \to 7$	$-1 \to 12$	$-1 \to 8$
k	$-1 \to 20$	$-3 \to 11$	$-11 \to 11$	$-17 \to 17$	$-1 \to 10$
l	$-23 \to 23$	$-41 \to 41$	$-19 \to 19$	$-25 \to 25$	$-13 \to 13$
No. of standard reflections (frequency)	3 (97)	3 (97)	3 (97)	3 (97)	3 (97)
Scan type	ω	ω	ω	ω	ω
Scan range (°)	0.92	0.92	1.70	1.06	0.92
No. of reflections collected [$I > 2\sigma(I)$]	6861	7371	4000	13606	2117
No. of independent reflections	5622	5436	3067	11639	1565
R_{int}	0.0472	0.0366	0.0671	0.0365	0.0620
No. of reflections observed [$I > 2\sigma(I)$]	3057	3682	1506	7666	1129
Data/restraints/parameters	5600/1/662	5433/0/345	3066/0/181	11605/0/757	1546/0/195
Goodness-of-fit on F^2	1.024	1.025	1.023	1.078	0.970
Final R indices [$I > 2\sigma(I)$], R_1	0.0714	0.0545	0.0764	0.0536	0.0693
R indices (all data), R_1	0.1421	0.0887	0.1551	0.0906	0.0906
wR_2	0.2499	0.1636	0.2314	0.1598	0.2010
$(\Delta/\sigma)_{max}$	0.416	-0.040	0.025	0.004	0.037
$(\Delta/\sigma)_{average}$	0.040	0.009	0.004	0.001	0.007
Weighting scheme		$1/[\sigma^2(F_o^2) + (dp)^2 + fp]$, where $p = [\max(F_o^2, 0) + 2F_c^2]/3$			
d	0.0958	0.0679	0.1025	0.063	0.1726
f	0.4900	0.6177	0.1068	1.3545	3.3255
Largest difference peak/hole (e Å⁻³)	0.160/−0.169	0.205/−0.160	0.202/−0.197	0.29/−0.19	0.18/−0.17
Method			Full-matrix least-squares on F^2		

squares refinements (*SHELXTL-Plus* and *SHELXL93*, Sheldrick, 1995). Methyl H atoms were located by means of ΔF syntheses with toroidal averaging, and were included in subsequent calculations as a group of idealized tetrahedral geometry riding on the methyl C atom. The positions of all other H atoms were calculated assuming standard geometries, and constrained to ride on their respective C atoms. For final refinements, all
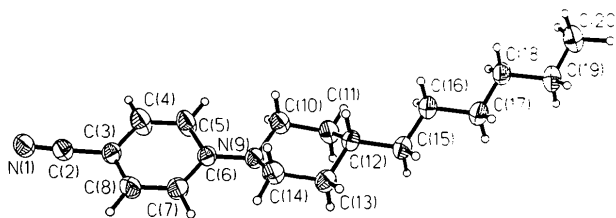

Fig. 1. *ORTEP*-like diagram of (I) ($n = 6$). Ellipsoids are drawn at the 50% probability level. Also shown is the atom numbering scheme used throughout. Note that the alkyl tails have similar and, in some homologs, smaller isotropic equivalent thermal parameters than the cyanophenyl moiety.

structures were refined on F^2 using all data, retaining $F^2 < 0$. For aesthetic convenience and familiarity, the unweighted discrepancy indices on F for those data where $I > 2\sigma(I)$ are provided and denoted R_1. Final atomic coordinates and equivalent isotropic displacement parameters are given in Tables 2–6 for (I) ($n = 4$–8), respectively.* Fig. 1 shows for a representative structure, (I) ($n = 6$), the atom labeling scheme employed throughout and the general disposition of the phenyl, piperidyl and alkyl moieties that comprise the family (I).

For (I) ($n = 4$), there are four molecules per asymmetric unit in space group $P2_1$, a number of sufficient size to warrant close inspection for missed symmetry. The cell is pseudo-orthorhombic [$\beta = 90.43\,(3)°$], with a pseudoscrew axis parallel to x which relates pairs of molecules, in addition to the screw axis of $P2_1$. However,

for equivalent data in an orthorhombic lattice, $R_{int} = 0.16$. Close inspection of precession-photo-like displays of the reciprocal lattice revealed no sign of glide planes. Refinement of the structure in $P2_1$ proceeded smoothly to convergence with the highest correlation coefficient being less than 0.6. Moreover, the differences in conformations are significant, and, in particular, for the apparently centrosymmetrically related pairs of molecules, A and B, and C and D, the piperidyl rings lack an inversion relationship. The alkyl chain of molecule A is disordered: the minor conformer [relative occupancy 0.14 (2)] involves disorder at the methylene site C(16A) and the methyl site C(18A).

For (I) ($n = 5$), structure elaboration in $P2_1/c$ ($Z = 8$) proceeded smoothly to convergence. A small number of reflections (17) showed weak but significant violation of the glide plane extinction [$2\sigma(I) < I < 5\sigma(I)$]. Development of the structure in space group $P2_1$ proceeded unsatisfactorily, even with damping of least-squares refinements by augmentation of diagonal elements of the least-squares matrix. Close inspection of the structure in $P2_1/c$ revealed no aberrations in stereochemistry or atomic displacement parameters. Thus, the crystal structure is appropriately described in space group $P2_1/c$, and the weakly observed reflections may be attributed to a minute disorder of the molecules in the crystal structure, but of a degree less than that seen for (I) ($n = 4$ and 7), where the disorder is of sufficient magnitude to lead to low symmetry space groups where the asymmetric unit comprises two pairs of conformationally similar molecules.

(I) ($n = 6$) was initially solved by direct methods and refined to $R_1 = 0.15$, with two overlapping disordered molecules. Fragment search (PATSEE), using (I) ($n = 5$) as a fragment, yielded a solution which refined to $R_1 = 0.0764$ for a model with no disorder. The correct solution was related to the incorrect disordered one by inversion of the mean coordinates of each pair of atoms, e.g. N(1) and N(1'), about the point ($\frac{1}{4}, 0, \frac{1}{4}$).

For (I) ($n = 7$), direct methods in $P1$ yielded a solution with two ordered and two disordered molecules in the asymmetric unit, which upon refinement led to R_1 (7666 data) $= 0.1077$ (11 562 data/150 restraints/1131 variables). Each ordered molecule had a pair of translationally disordered molecules whose average coordinates in x and y were approximately equal to those of the ordered molecule, while the average z coordinate differed by approximately 0.5. In the light of experiences with (I) ($n = 6$), considerable efforts were made by means of vector-search methods, PATSEE, forced relocation of molecules, and alternative direct-methods strategies to obtain an ordered structure. The relationship between disordered and ordered models for (I) ($n = 6$) was inspected for possible application to the apparent disorder afflicting (I) ($n = 7$). As is detailed below, no such application is possible, not least because for (I) ($n = 6$) there is only one molecule in the asymmetric

Table 2. *Atomic coordinates* ($\times 10^4$) *and equivalent isotropic displacement parameters* ($\mathring{A}^2 \times 10^3$) *for* (I) ($n = 4$)

$$U_{eq} = (1/3)\sum_i \sum_j U_{ij} a_i^* a_j^* \mathbf{a}_i.\mathbf{a}_j.$$

	x	y	z	U_{eq}
N(1A)	1106 (10)	8134 (6)	2033 (4)	84 (3)
C(2A)	1130 (11)	7495 (7)	1880 (5)	68 (3)
C(3A)	1182 (9)	6719 (6)	1696 (4)	59 (2)
C(4A)	1222 (9)	6495 (6)	1037 (4)	62 (2)
C(5A)	1268 (9)	5741 (6)	868 (4)	57 (2)
C(6A)	1269 (9)	5135 (7)	1325 (4)	58 (3)
C(7A)	1256 (9)	5363 (5)	2015 (4)	60 (2)
C(8A)	1232 (9)	6133 (6)	2187 (4)	65 (3)
N(9A)	1416 (7)	4369 (4)	1168 (3)	53 (2)
C(10A)	957 (9)	4152 (6)	470 (4)	66 (2)
C(11A)	1515 (9)	3363 (5)	297 (3)	59 (2)
C(12A)	985 (8)	2748 (5)	794 (4)	57 (2)
C(13A)	1512 (8)	2997 (5)	1461 (4)	52 (2)
C(14A)	1015 (10)	3789 (5)	1662 (4)	66 (2)
C(15A)	1587 (9)	1934 (6)	594 (4)	67 (2)
C(16A)	892 (10)	1283 (6)	1000 (4)	53 (3)
C(17A)	1546 (11)	495 (6)	806 (5)	73 (3)
C(18A)	792 (14)	−147 (7)	1165 (5)	78 (4)
N(1D)	−1112 (10)	5735 (7)	4542 (4)	87 (3)
C(2D)	−1102 (9)	6388 (7)	4431 (5)	62 (3)
C(3D)	−1140 (8)	7195 (6)	4266 (4)	58 (2)
C(4D)	−1107 (9)	7756 (6)	4734 (4)	63 (2)
C(5D)	−1140 (9)	8506 (6)	4565 (4)	62 (3)
C(6D)	−1194 (8)	8766 (6)	3908 (4)	46 (2)
C(7D)	−1252 (9)	8171 (7)	3416 (5)	68 (3)
C(8D)	−1208 (9)	7417 (7)	3598 (4)	67 (3)
N(9D)	−1173 (7)	9509 (5)	3727 (3)	60 (2)
C(10D)	−1665 (9)	10109 (6)	4217 (4)	67 (2)
C(11D)	−1181 (9)	10878 (6)	4052 (4)	67 (3)
C(12D)	−1601 (9)	11160 (6)	3336 (4)	64 (2)
C(13D)	−1069 (10)	10546 (7)	2858 (4)	75 (3)
C(14D)	−1522 (11)	9742 (6)	3027 (4)	75 (3)
C(15D)	−1027 (8)	11924 (6)	3157 (4)	64 (2)
C(16D)	−1653 (8)	12622 (6)	3536 (4)	64 (2)
C(17D)	−1058 (11)	13370 (7)	3322 (5)	81 (3)
C(18D)	−1653 (13)	14082 (7)	3684 (5)	101 (3)
N(1C)	6344 (10)	688 (6)	512 (4)	80 (2)
C(2C)	6348 (9)	1336 (7)	628 (5)	64 (3)
C(3C)	6347 (8)	2153 (6)	792 (5)	62 (3)
C(4C)	6289 (9)	2716 (6)	319 (4)	62 (3)
C(5C)	6293 (9)	3459 (6)	478 (4)	59 (2)
C(6C)	6302 (8)	3722 (6)	1139 (4)	46 (2)
C(7C)	6378 (9)	3129 (7)	1639 (4)	61 (3)
C(8C)	6406 (9)	2367 (7)	1467 (4)	67 (3)
N(9C)	6350 (7)	4469 (5)	1327 (3)	52 (2)
C(10C)	5962 (10)	5040 (6)	824 (4)	70 (3)
C(11C)	6440 (9)	5831 (6)	993 (4)	67 (3)
C(12C)	5919 (8)	6112 (5)	1708 (3)	54 (2)
C(13C)	6423 (11)	5493 (6)	2189 (4)	79 (3)
C(14C)	5904 (9)	4705 (5)	2003 (3)	59 (2)
C(15C)	6440 (9)	6896 (5)	1894 (4)	63 (3)
C(16C)	5883 (8)	7568 (5)	1483 (4)	59 (2)
C(17C)	6342 (10)	8333 (6)	1730 (4)	68 (3)
C(18C)	5688 (12)	9004 (6)	1334 (5)	95 (3)
N(1B)	3692 (9)	3304 (7)	2943 (4)	82 (2)
C(2B)	3717 (11)	2682 (7)	3078 (5)	64 (3)
C(3B)	3864 (8)	1906 (6)	3244 (4)	54 (2)
C(4B)	3781 (8)	1639 (6)	3906 (4)	55 (2)
C(5B)	3738 (9)	889 (6)	4068 (4)	59 (3)
C(6B)	3756 (9)	316 (6)	3592 (4)	52 (2)
C(7B)	3695 (8)	550 (6)	2900 (4)	55 (2)
C(8B)	3700 (8)	1316 (6)	2744 (4)	60 (2)
N(9B)	3826 (7)	−465 (5)	3753 (3)	54 (2)
C(10B)	3496 (11)	−668 (6)	4447 (4)	78 (3)
C(11B)	4032 (10)	−1461 (6)	4622 (4)	66 (3)
C(12B)	3454 (9)	−2084 (5)	4129 (4)	60 (2)
C(13B)	3913 (10)	−1848 (6)	3441 (4)	69 (3)
C(14B)	3343 (9)	−1033 (5)	3266 (4)	62 (2)
C(15B)	4108 (8)	−2868 (6)	4332 (4)	65 (2)
C(16B)	3453 (9)	−3528 (6)	3917 (4)	66 (2)

Table 2 (*cont.*)

	x	y	z	U_{eq}
C(17B)	3985 (12)	−4323 (7)	4169 (5)	80 (3)
C(18B)	3217 (13)	−4975 (7)	3839 (5)	102 (3)
C(16W)†	1872 (149)	1416 (76)	1190 (93)	161 (42)
C(18W)†	2227 (196)	−126 (98)	1265 (67)	224 (64)

† See text.

Table 3. Atomic coordinates ($\times 10^4$) and equivalent isotropic displacement parameters ($\mathring{A}^2 \times 10^3$) for (I) ($n = 5$)

$$U_{eq} = (1/3)\sum_i\sum_j U_{ij}a_i^* a_j^* \mathbf{a}_i.\mathbf{a}_j.$$

	x	y	z	U_{eq}
N(1A)	−2003 (2)	527 (2)	3233 (1)	58 (1)
C(2A)	−2644 (2)	352 (2)	2934 (1)	42 (1)
C(3A)	−3445 (2)	135 (2)	2561 (1)	36 (1)
C(4A)	−3797 (2)	1217 (2)	2309 (1)	39 (1)
C(5A)	−4562 (2)	1008 (2)	1953 (1)	37 (1)
C(6A)	−5051 (2)	−309 (2)	1825 (1)	32 (1)
C(7A)	−4659 (2)	−1396 (2)	2083 (1)	37 (1)
C(8A)	−3897 (2)	−1180 (2)	2440 (1)	38 (1)
N(9A)	−5885 (2)	−522 (2)	1476 (1)	34 (1)
C(10A)	−6137 (2)	631 (2)	1206 (1)	38 (1)
C(11A)	−7404 (2)	366 (2)	891 (1)	38 (1)
C(12A)	−7244 (2)	−978 (2)	681 (1)	35 (1)
C(13A)	−7107 (2)	−2109 (2)	981 (1)	41 (1)
C(14A)	−5827 (3)	−1872 (2)	1290 (1)	43 (1)
C(15A)	−8516 (2)	−1201 (2)	362 (1)	40 (1)
C(16A)	−8405 (2)	−2492 (2)	123 (1)	41 (1)
C(17A)	−9634 (2)	−2635 (2)	−208 (1)	41 (1)
C(18A)	−9471 (3)	−3875 (3)	−459 (1)	49 (1)
C(19A)	−10718 (3)	−4034 (3)	−785 (1)	67 (1)
N(1B)	4445 (2)	2906 (2)	5183 (1)	61 (1)
C(2B)	3769 (2)	3141 (3)	4892 (1)	46 (1)
C(3B)	2933 (2)	3460 (2)	4528 (1)	38 (1)
C(4B)	2816 (2)	4802 (2)	4400 (1)	42 (1)
C(5B)	2034 (2)	5119 (2)	4050 (1)	39 (1)
C(6B)	1313 (2)	4102 (2)	3814 (1)	32 (1)
C(7B)	1446 (2)	2739 (2)	3948 (1)	39 (1)
C(8B)	2231 (2)	2433 (2)	4298 (1)	42 (1)
N(9B)	451 (2)	4409 (2)	3468 (1)	32 (1)
C(10B)	396 (2)	5837 (2)	3337 (1)	38 (1)
C(11B)	−851 (2)	6081 (2)	3018 (1)	37 (1)
C(12B)	−794 (2)	5115 (2)	2679 (1)	33 (1)
C(13B)	−786 (2)	3658 (2)	2836 (1)	38 (1)
C(14B)	470 (2)	3420 (2)	3154 (1)	41 (1)
C(15B)	−2059 (2)	5376 (2)	2360 (1)	35 (1)
C(16B)	−1977 (2)	4592 (2)	1987 (1)	37 (1)
C(17B)	−3282 (2)	4878 (2)	1687 (1)	40 (1)
C(18B)	−3255 (3)	4100 (2)	1314 (1)	46 (1)
C(19B)	−4600 (3)	4362 (3)	1024 (1)	66 (1)

Table 4. Atomic coordinates ($\times 10^4$) and equivalent isotropic displacement parameters ($\mathring{A}^2 \times 10^3$) for (I) ($n = 6$)

$$U_{eq} = (1/3)\sum_i\sum_j U_{ij}a_i^* a_j^* \mathbf{a}_i.\mathbf{a}_j.$$

	x	y	z	U_{eq}
N(1)	2806 (5)	−4695 (3)	5464 (2)	51 (1)
C(2)	2621 (5)	−3868 (3)	5006 (2)	39 (1)
C(3)	2341 (5)	−2782 (3)	4466 (2)	37 (1)
C(4)	350 (6)	−2397 (4)	4240 (3)	59 (1)
C(5)	58 (6)	−1323 (4)	3760 (3)	57 (1)
C(6)	1739 (5)	−563 (3)	3483 (2)	34 (1)
C(7)	3730 (6)	−990 (4)	3699 (3)	60 (1)
C(8)	4033 (6)	−2078 (4)	4176 (3)	60 (1)
N(9)	1460 (4)	520 (3)	2981 (2)	35 (1)
C(10)	−703 (5)	891 (3)	2806 (2)	42 (1)
C(11)	−892 (5)	1866 (3)	2130 (2)	45 (1)
C(12)	573 (5)	3333 (3)	2462 (2)	38 (1)
C(13)	2802 (5)	2864 (4)	2568 (2)	45 (1)
C(14)	3029 (5)	1872 (3)	3237 (2)	46 (1)
C(15)	367 (5)	4382 (4)	1818 (2)	45 (1)
C(16)	−1813 (5)	4995 (3)	1763 (2)	44 (1)
C(17)	−1975 (6)	6138 (4)	1185 (2)	48 (1)
C(18)	−4146 (6)	6750 (4)	1156 (2)	46 (1)
C(19)	−4367 (6)	7875 (4)	567 (2)	52 (1)
C(20)	−6540 (7)	8491 (4)	566 (3)	66 (1)

of placing some faith in the original diffraction data: final discrepancy indices should approach the discrepancy index for the merging of equivalent data, unless there is a compelling reason for the difference, such as missing electron density.

For (I) ($n = 8$), PATSEE yielded a solution that refined satisfactorily to $R = 0.09$. The piperidyl ring was almost planar, but with two C atoms at the 2- and 5-positions relative to the nitrogen showing exaggerated atomic displacement parameters and the C atom at the 4-position showing lesser displacement. The disorder was modeled by assuming two chair conformations of the piperidyl ring involving flip-flops of atoms C(11) and C(14). Several H atoms (including half H atoms) were visible in the difference Fourier map in positions congruent with this model. For final refinements, H atoms were placed at their calculated positions and allowed to ride on their attached C atoms. Least-squares refinements converged at $R_1 = 0.069$. Bond angles at the 1- and 4-positions of the piperidyl ring deviate from those seen in other piperidyl rings of the family (I), indicating that the disorder propagates beyond atoms C(11) and C(14). In view of the disorder, solution and refinement of the crystal structure in space group $P2_1$ were investigated, since there were a number of weak but significant violations of the glide plane extinction. The piperidyl ring remained disordered in both molecules, and even with mild damping applied, all the hallmarks of a missing inversion center were present. Therefore, the mildly disordered structure in $P2_1/c$ represents the best solution to the data. Violations of the glide plane extinction rule are attributed to the same cause as in (I) ($n = 5$), *vide supra*. Although this data set is the only one to be collected with copper radiation, and the collection was not extended to higher angle because of the constraints of the low temperature device, the rapid

unit, whereas for (I) ($n = 7$) there are four molecules, which need not share a common misplaced origin. Eventually, in space group $P1$, a nondisordered solution emerged, that on refinement converged at $R_1 = 0.08$. Centrosymmetric relationships among pairs of molecules were obvious not only from the coordinates, but also from the large number of correlation coefficients in excess of 0.85. With the molecules now correctly positioned in $P\bar{1}$, least-squares refinements converged satisfactorily at $R_1 = 0.0536$. In the ordered correct model, pairs of molecules are also approximately related by $z + \frac{1}{2}$. Relative to the disordered incorrect model, one pair of molecules differs by 0.75 in z, whereas the other pair differs by 0.25 in z. The crystal structures of (I) ($n = 6$ and 7) provide a salutary lesson in the importance

Table 5. *Atomic coordinates* $(\times 10^4)$ *and equivalent isotropic displacement parameters* $(\text{Å}^2 \times 10^3)$ *for* (I) $(n = 7)$

$$U_{eq} = (1/3) \sum_i \sum_j U_{ij} a_i^* a_j^* \mathbf{a}_i . \mathbf{a}_j.$$

	x	y	z	U_{eq}
N(1A)	1608 (2)	−5187 (1)	−2396 (1)	50 (1)
C(2A)	1713 (2)	−4842 (2)	−1840 (1)	38 (1)
C(3A)	1845 (2)	−4411 (1)	−1141 (1)	34 (1)
C(4A)	804 (2)	−4196 (1)	−912 (1)	38 (1)
C(5A)	936 (2)	−3810 (1)	−241 (1)	36 (1)
C(6A)	2104 (2)	−3618 (1)	231 (1)	32 (1)
C(7A)	3145 (2)	−3818 (2)	−10 (1)	36 (1)
C(8A)	3008 (2)	−4210 (2)	−683 (1)	39 (1)
N(9A)	2199 (2)	−3221 (1)	908 (1)	33 (1)
C(10A)	1217 (2)	−3690 (2)	1159 (1)	38 (1)
C(11A)	1203 (2)	−3140 (2)	1853 (1)	37 (1)
C(12A)	2503 (2)	−2869 (2)	2344 (1)	35 (1)
C(13A)	3449 (2)	−2366 (2)	2064 (1)	37 (1)
C(14A)	3462 (2)	−2948 (2)	1373 (1)	35 (1)
C(15A)	2447 (2)	−2328 (2)	3041 (1)	39 (1)
C(16A)	3666 (2)	−2084 (2)	3592 (1)	41 (1)
C(17A)	3462 (2)	−1710 (2)	4281 (1)	40 (1)
C(18A)	4664 (2)	−1388 (2)	4847 (1)	41 (1)
C(19A)	4440 (2)	−1043 (2)	5535 (1)	41 (1)
C(20A)	5630 (2)	−702 (2)	6102 (1)	46 (1)
C(21A)	5377 (3)	−372 (2)	6784 (1)	56 (1)
N(1B)	−1212 (2)	544 (2)	−2469 (1)	59 (1)
C(2B)	−777 (2)	715 (2)	−1910 (1)	44 (1)
C(3B)	−251 (2)	943 (2)	−1205 (1)	38 (1)
C(4B)	−881 (2)	1365 (2)	−758 (1)	43 (1)
C(5B)	−397 (2)	1578 (2)	−83 (1)	40 (1)
C(6B)	753 (2)	1388 (2)	184 (1)	38 (1)
C(7B)	1360 (2)	947 (2)	−282 (1)	49 (1)
C(8B)	882 (2)	740 (2)	−956 (1)	46 (1)
N(9B)	1283 (2)	1663 (1)	863 (1)	41 (1)
C(10B)	497 (2)	1939 (2)	1319 (1)	56 (1)
C(11B)	1284 (2)	2510 (2)	2014 (1)	47 (1)
C(12B)	2238 (2)	2054 (2)	2307 (1)	37 (1)
C(13B)	3042 (2)	1797 (2)	1816 (1)	47 (1)
C(14B)	2253 (2)	1233 (2)	1119 (1)	46 (1)
C(15B)	3079 (2)	2630 (2)	2994 (1)	45 (1)
C(16B)	2380 (2)	2903 (2)	3531 (1)	42 (1)
C(17B)	3278 (2)	3326 (2)	4225 (1)	42 (1)
C(18B)	2637 (2)	3562 (2)	4786 (1)	42 (1)
C(19B)	3589 (2)	3919 (2)	5469 (1)	43 (1)
C(20B)	3019 (2)	4085 (2)	6056 (1)	49 (1)
C(21B)	4015 (3)	4450 (2)	6718 (1)	62 (1)
N(1C)	1486 (2)	−5085 (2)	2438 (1)	51 (1)
C(2C)	1587 (2)	−4764 (2)	2996 (1)	40 (1)
C(3C)	1728 (2)	−4370 (1)	3700 (1)	35 (1)
C(4C)	2875 (2)	−4243 (2)	4156 (1)	40 (1)
C(5C)	3005 (2)	−3901 (2)	4832 (1)	38 (1)
C(6C)	1976 (2)	−3677 (1)	5080 (1)	32 (1)
C(7C)	838 (2)	−3786 (1)	4610 (1)	35 (1)
C(8C)	711 (2)	−4123 (1)	3939 (1)	35 (1)
N(9C)	2058 (2)	−3343 (1)	5762 (1)	32 (1)
C(10C)	3299 (2)	−3162 (2)	6226 (1)	37 (1)
C(11C)	3298 (2)	−2638 (2)	6933 (1)	37 (1)
C(12C)	2290 (2)	−3149 (2)	7178 (1)	35 (1)
C(13C)	1010 (2)	−3343 (2)	6679 (1)	39 (1)
C(14C)	1025 (2)	−3829 (2)	5973 (1)	40 (1)
C(15C)	2230 (2)	−2631 (2)	7875 (1)	38 (1)
C(16C)	3446 (2)	−2381 (2)	8431 (1)	39 (1)
C(17C)	3266 (2)	−1921 (2)	9112 (1)	38 (1)
C(18C)	4482 (2)	−1554 (2)	9671 (1)	40 (1)
C(19C)	4282 (2)	−1105 (2)	10348 (1)	40 (1)
C(20C)	5489 (2)	−694 (2)	10908 (1)	45 (1)
C(21C)	5263 (3)	−246 (2)	11575 (1)	63 (1)
N(1D)	1294 (2)	−606 (2)	7600 (1)	61 (1)
C(2D)	871 (2)	−754 (2)	7044 (1)	44 (1)
C(3D)	353 (2)	−955 (2)	6337 (1)	38 (1)
C(4D)	995 (2)	−1340 (2)	5887 (1)	40 (1)
C(5D)	532 (2)	−1520 (2)	5214 (1)	39 (1)
C(6D)	−630 (2)	−1344 (1)	4955 (1)	34 (1)
C(7D)	−1261 (2)	−935 (2)	5423 (1)	44 (1)
C(8D)	−786 (2)	−751 (2)	6093 (1)	44 (1)

Table 5 (cont.)

	x	y	z	U_{eq}
N(9D)	−1158 (2)	−1583 (1)	4275 (1)	36 (1)
C(10D)	−363 (2)	−1848 (2)	3820 (1)	44 (1)
C(11D)	−1150 (2)	−2380 (2)	3112 (1)	41 (1)
C(12D)	−2067 (2)	−1878 (2)	2838 (1)	37 (1)
C(13D)	−2865 (2)	−1630 (2)	3329 (1)	46 (1)
C(14D)	−2085 (2)	−1110 (2)	4033 (1)	44 (1)
C(15D)	−2908 (2)	−2431 (2)	2145 (1)	44 (1)
C(16D)	−2220 (2)	−2728 (2)	1611 (1)	41 (1)
C(17D)	−3123 (2)	−3171 (2)	919 (1)	41 (1)
C(18D)	−2495 (2)	−3462 (2)	359 (1)	40 (1)
C(19D)	−3450 (2)	−3844 (2)	−320 (1)	41 (1)
C(20D)	−2896 (2)	−4105 (2)	−910 (1)	50 (1)
C(21D)	−3905 (3)	−4495 (2)	−1569 (1)	60 (1)

Table 6. *Atomic coordinates* $(\times 10^4)$ *and equivalent isotropic displacement parameters* $(\text{Å}^2 \times 10^3)$ *for* (I) $(n = 8)$

$$U_{eq} = (1/3) \sum_i \sum_j U_{ij} a_i^* a_j^* \mathbf{a}_i . \mathbf{a}_j.$$

	x	y	z	U_{eq}
N(1)	−150 (4)	1499 (4)	138 (4)	83 (2)
C(2)	184 (4)	1227 (4)	947 (4)	63 (2)
C(3)	592 (4)	915 (4)	1950 (3)	50 (1)
C(4)	660 (4)	1770 (4)	2686 (4)	55 (1)
C(5)	1027 (4)	1492 (4)	3658 (3)	54 (1)
C(6)	1359 (4)	317 (4)	3965 (3)	47 (1)
C(7)	1296 (4)	−544 (4)	3209 (3)	53 (1)
C(8)	923 (4)	−256 (4)	2233 (3)	55 (1)
N(9)	1719 (3)	19 (3)	4945 (3)	54 (1)
C(10)	1845 (5)	968 (4)	5682 (3)	64 (2)
C(12)	2485 (6)	−532 (5)	7039 (3)	90 (2)
C(13)	2286 (5)	−1492 (4)	6269 (3)	64 (2)
C(11A)†	2382 (9)	659 (9)	6657 (7)	56 (2)
C(14A)†	1712 (10)	−1171 (9)	5231 (7)	60 (2)
C(11B)†	1812 (10)	498 (9)	6746 (7)	56 (2)
C(14B)†	2426 (10)	−1069 (9)	5269 (7)	60 (2)
C(15)	2720 (4)	−930 (4)	8068 (3)	61 (2)
C(16)	2891 (5)	0 (5)	8870 (3)	67 (2)
C(17)	3227 (4)	−464 (4)	9907 (3)	62 (2)
C(18)	3386 (5)	503 (5)	10687 (3)	66 (2)
C(19)	3779 (4)	71 (4)	11735 (3)	59 (2)
C(20)	3910 (4)	1056 (4)	12496 (3)	59 (2)
C(21)	4273 (4)	641 (5)	13553 (3)	65 (2)
C(22)	4380 (5)	1650 (5)	14284 (4)	83 (2)

† Disordered; see text.

fall-off in diffraction intensity as the 2θ limit of 97.5° was approached indicates that true resolution of the disorder of the piperidyl is probably unlikely with molybdenum radiation; for all the other homologues except (I) $(n = 6)$, at the limits of data collection with molybdenum radiation $(2\theta \sim 50°)$, the proportion of data above background was small.

Results

Molecular structure

Table 7 lists for each of the homologs of (I) a selection of bond lengths and angles that might be sensitive to crystal packing effects or delocalization effects in the piperidylcyanobenzonitrile moiety. With few exceptions, which will be described below, bond distances and angles among formally chemically equivalent atoms maintain constant values for all 12 crystallographically

Table 7. *Selected average bond distances (Å) and angles (°) for all molecules of (I) (n = 4–8);
see Fig. 1 for atom labeling*

(I) (n =)	N(1)— C(2)— C(3)	C(4)— C(3)— C(8)	Δ[C(2)— C(3)— C(4/8)]*	C(2)— C(3)	C(3/3)— C(4/8)†		C(4/7)— C(5/8)		C(5/6)— C(6/7)		C(6)— N(9)	C(5)— C(6)— C(7)	Δ[C(5/7)— C(6)— N(9)]	C(10)— N(9)— C(14)	Δ[C(6)— N(9)— C(10/14)]
4A	179 (1)	117	1	1.40 (1)	1.38	1.42	1.36	1.39	1.40	1.44	1.38	115	6	114	4
4B	177 (1)	118	4	1.45 (1)	1.36	1.39	1.35	1.36	1.39	1.43	1.35	115	5	112	1
4C	179 (1)	118	5	1.46 (1)	1.36	1.40	1.33	1.37	1.40	1.44	1.36	115	6	113	3
4D	179 (1)	115	1	1.39 (1)	1.40	1.44	1.33	1.37	1.38	1.44	1.40	117	3	115	3
5A	179.9 (2)	117.8	0.8	1.437 (3)	1.389	1.397	1.372	1.371	1.413	1.412	1.376	115.7	0.5	113.9	0.0
5B	178.9 (2)	118.6	0.8	1.438 (3)	1.384	1.393	1.372	1.375	1.403	1.411	1.394	116.9	1.6	113.0	0.9
6	177.3 (3)	117.8	0.8	1.442 (4)	1.380	1.374	1.371	1.379	1.385	1.391	1.400	115.8	0.7	114.0	0.7
7A	179.8 (3)	118.7	0.3	1.443 (3)	1.398	1.387	1.377	1.381	1.406	1.403	1.399	117.3	2.7	112.1	3.3
7B	178.7 (3)	118.6	1.2	1.440 (3)	1.390	1.391	1.376	1.373	1.408	1.410	1.382	115.9	0.6	113.6	0.3
7C	179.0 (3)	118.7	0.3	1.444 (3)	1.391	1.398	1.380	1.370	1.407	1.405	1.401	117.1	1.8	111.9	3.1
7D	178.8 (3)	118.4	0.8	1.448 (3)	1.385	1.394	1.376	1.372	1.404	1.414	1.387	116.3	0.7	113.2	0.6
8‡	178.9 (6)	117.6	0.8	1.420 (7)	1.384	1.392	1.365	1.373	1.404	1.411	1.380	115.8	0.3	119 (1)	1 (1)
														114 (1)	3 (1)

* Difference in bond angles C(2)—C(3)—C(4) and C(2)—C(3)—C(8); similarly for other bond angles prefaced by Δ.
† Bond distances C(3)—C(4) and C(3)—C(8); similarly for other pairs of formally chemically equivalent bond distances.
‡ Piperidyl ring is disordered; parameters involving piperidyl atoms have higher errors and lower accuracy.

independent molecules distributed over five homologs. Considerable torsional flexibility is observed, however, as illustrated in Fig. 2 and enumerated in Table 8.

The cyano moiety is linear to within 2.7 (2)°, although significant tilting is observed, with differences in the NC—C—C$_{phenyl}$ angles ranging from 0.3 (2) to 5 (1)° and displacements of the cyano carbon from the plane of the phenyl ring as large as 0.071 Å, (I) (n = 6). Additionally, displacements of the piperidyl N atoms from the phenyl planes as large as 0.104 [molecule B of I
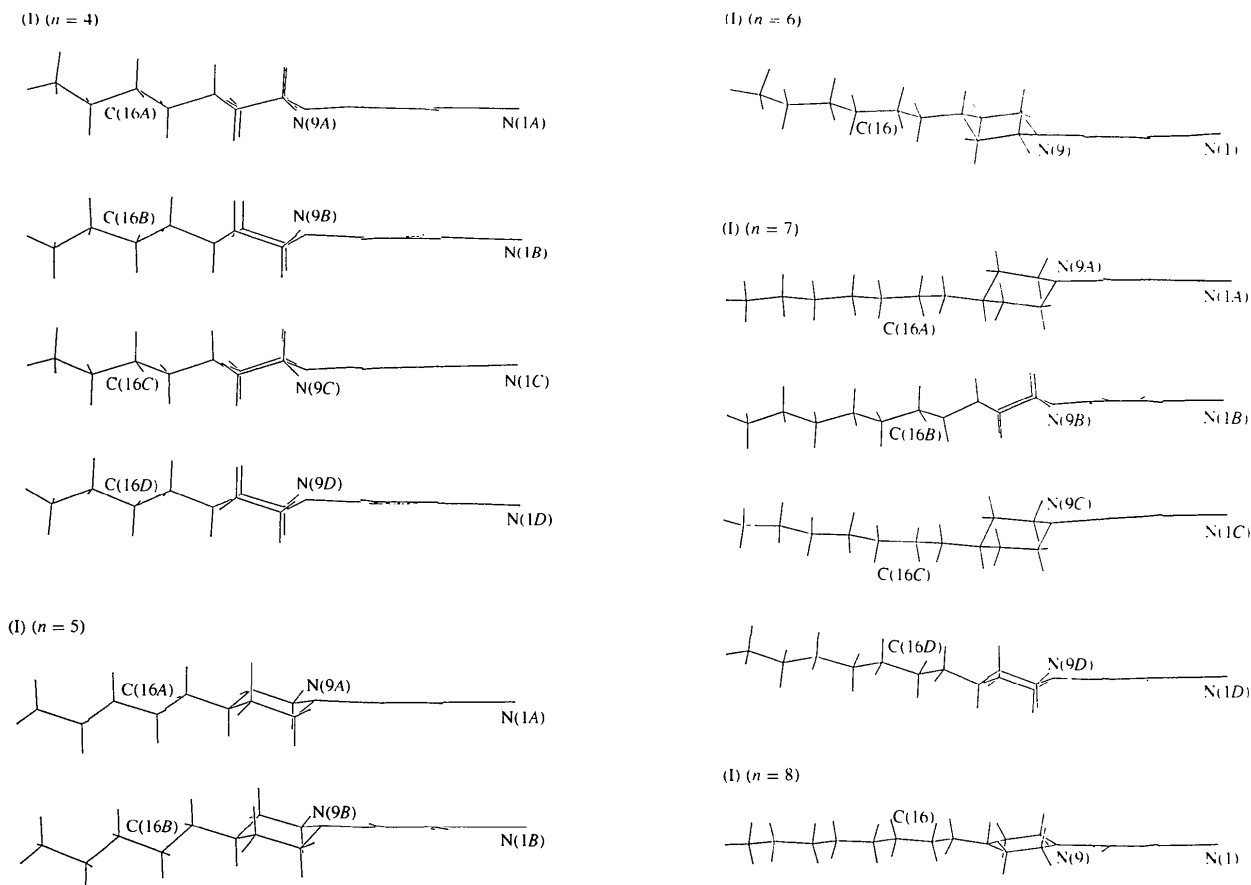

Fig. 2. Line diagrams of all molecules of (I) from a common orientation. When rotated 90° about the cyanophenyl moiety, all molecules have atoms C(4), C(5), C(10), C(11) and C(16) on the same (lower) side of the molecule. Thus, atom C(16) is projected out of the plane of the page.

Table 8. *Angles* (°) *among various planes* (*defined and denoted below*)

Phenyl plane (Ph); the line connecting atoms C(10) and C(14) at positions 2 and 6 of the piperidyl group (L); the plane defined by the alkyl tail (Al); the plane defined by piperidyl C atoms C(10), C(11), C(13) and C(14) (Pip); pyramidalization of the amino N atom (Py), where P is the displacement (in Å) of the amino N atom from the plane defined by atoms C(6), C(10) and C(14); the displacement of the amino N atom from the plane of the phenyl ring (P_N). The angle between Ph and L is approximately the angle between the *p*-orbital of the *ipso*-phenyl C atom and the lone-pair orbital of the amino N atom. See Fig. 1 for atom labeling. All planes determined by unweighted least-squares.

(I) (n =)	Ph/L*	Ph/Pip*	Ph/Al*	Pip/Al*	Py (Å)†	P_N (Å)†
4A	1	16	43	41	0.274	0.081
4B	2	18	38	35	0.243	0.089
4C	3	17	33	34	0.238	0.043
4D	5	17	43	35	0.227	0.051
5A	10	21	44	32	0.236	0.074
5B	17	23	58	38	0.287	0.070
6	19	21	14	33	0.306	0.011
7A	28	30	6	28	0.333	0.006
7B	3	23	24	28	0.240	0.104
7C	28	30	10	22	0.341	0.035
7D	5	22	23	26	0.252	0.100
8A‡	(−)12	14	6	11	0.104	0.021
8A‡	(+)8	24	6	25	0.187	0.021
DMABN§	3				0.072	

* Except for (I) (n = 8), estimated maximum error ±1°.

† Except for (I) (n = 8), estimated maximum error ±0.005 Å.

‡ Disordered piperidyl ring; twist and pyramidalization parameters underestimated.

§ N,N-Dimethylamino-*p*-benzonitrile at 103 K (Jameson, Sheikh-Ali & Weiss, 1994).

(n = 7)] are observed. All the C atoms of the phenyl rings are displaced by less than 0.025 Å from the least-squares plane defined by them. This is despite substantial distortions at the carbon *ipso* to the cyano group [range 115 (1)–118.7 (3)°], at the carbon *ipso* to the piperidyl group [range 115 (1)–117.3 (3)°], and in the bond lengths around the phenyl ring where the ordering (H)C—C(H) < (NC)C—C < (pip)C—C is found. This pattern is also seen in N,N-dimethylamino-*p*-benzonitrile (Jameson, Sheikh-Ali & Weiss, 1994).

Selected conformational details are summarized in Table 8. A number of interesting correlations exist. The twist of the piperidyl ring with respect to the phenyl ring, as defined by the angle between the phenyl ring and the line C(10)···C(14) across the piperidyl ring, engenders significant differences in pairs of angles of the types $C_{phenyl}—C_{phenyl}—N_{pip}$, and $C_{pip}—C_{pip}—N_{pip}$. More significantly, this twist is correlated with the pyramidalization at the piperidyl nitrogen, as defined by the displacement of this N atom from the three-atom plane of the attached C atoms, C(6), C(10) and C(14): specifically, greater pyramidalization is correlated with (i) a greater twisting, (ii) a smaller displacement of the piperidyl N atom from the plane of the phenyl ring, (iii) a greater internal bond angle at the *ipso* phenyl carbon, (iv) a smaller internal bond angle at the piperidyl N atom, and (v) a longer $C_{phenyl}—N_{pip}$ bond length [as is especially apparent for the I (n = 7) homolog]. Such

observations are consistent with notions that conjugation of the piperidyl N atom with the phenyl ring is weakened by twisting of the piperidyl ring and by increased pyramidalization at the piperidyl N atom. Relative to the less constrained N,N-dimethylamino-*p*-benzonitrile, the piperidyl ring puckering inhibits planarity at the nitrogen and delocalization of the amino N atom with the phenyl ring. Comparison of the inductive electron-donating abilities (Lowry & Richardson, 1987) of the dimethylamino group ($\sigma_I = 0.06$) and of an alkyl group ($\sigma_I = -0.05$) indicates that molecules of (I) would be less polar than those of the analogous *trans*-1-alkyl-4-(4-cyanophenyl)cyclohexanes (II) if the amino–phenyl interaction were purely inductive.

All methylene groups have C—C—C bond angles in the range 112–119° with the largest angles found for the methylene group closest to the piperidyl ring. In all homologs, alkyl chains are all-*transoid* and planar to within 0.09 Å, although bond angles alternate in a small (1–3°) but significant way. These deviations must be included in any attempt to model accurately the packing properties of extended alkyl chains. Relative to the piperidyl ring, the alkyl chains are projected in a generally similar manner among the homologs; relative to the phenyl ring there is a much larger variation (see Table 8). The angles between the planes defined by the phenyl and alkyl tail C atoms are significantly smaller for (I) than that reported for *trans*-1-(4-cyanophenyl)-4-octylcyclohexane, where the corresponding value is 82° (Paulus & Haase, 1983). The propyl homolog of (II) adopts a molecular conformation and packing in its crystalline state that is very similar to *trans*-1-(4-cyanophenyl)-4-octylcyclohexane (Furmanova & Timofeeva, 1986).

Crystal packing

A surprising diversity of packing arrangements characterizes the crystal stuctures of the homologs of (I): three different space groups occur, and the asymmetric units consist of one, two or four molecules.
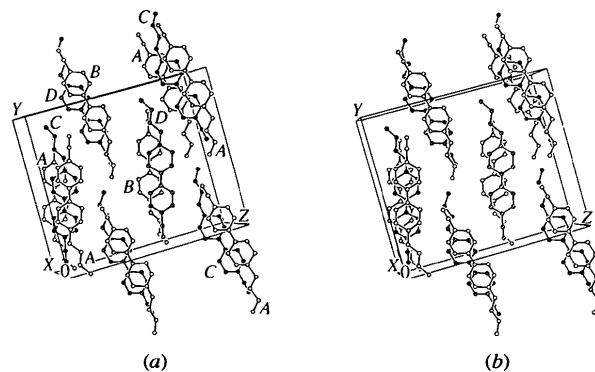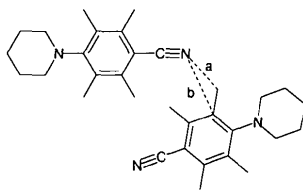

(a)   *(b)*

Fig. 3. Stereodiagram of the packing of (I) (n = 4), viewed approximately down the *a* axis, showing the stacking of molecules.

Table 9. *Closest intermolecular ring–ring contacts* (Å) *of crystalline* (I); *see Fig.* 1 *for atom labeling*


(*a*) Contacts between cyano nitrogen and phenyl C atoms *meta* to the cyano substituent.

(I) ($n =$)	a (Å)	b (Å)	Atoms in contact	Symmetry operation*
4	2.71	3.40	N(1A)···C(7D)	x, y, z
	2.85	3.46	N(1B)···C(7C)	x, y, z
	2.73	3.42	B(1C)···C(5A)	$1 - x, -\frac{1}{2} + y, -z$
	2.85	3.56	N(1D)···C(5B)	$-x, \frac{1}{2} + y, 1 - z$
8	2.87	3.56	N(1)···C(5″)	$x, \frac{1}{2} - y, -\frac{1}{2} + z$
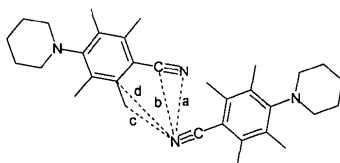
(*b*) Contacts between pairs of cyanophenyl moieties.

(I) ($n =$)	a (Å)	b (Å)	c (Å)	d (Å)	N···H—C	Atoms in contact of type a	Symmetry operation*
5	4.43	4.20	2.60	3.52 [C(4B)]	161	N(1B)···N(1B′)	$1 - x, 1 - y, 1 - z$
6	3.20	3.29	3.05	3.79 [C(8)]	134	N(1)···N(1″)	$1 - x, -1 - y, 1 - z$
	3.70	3.58	2.50	3.37 [C(4)]	151	N(1)···N(1′)	$-x, -1 - y, 1 - z$
7	3.51	3.50	2.68	3.55 [C(8C)]	151	N(1A)···N(1C)	$-x, -1 - y, -z$
	3.51	3.49	2.63	3.50 [C(4A)]	151	N(1C)···N(1A)	$-x, -1 - y, -z$
	3.57	3.46	2.51	3.38 [C(8D)]	151	N(1B)···N(1D)	$x, y, -1 + z$
	3.57	3.48	2.52	3.42 [C(8B)]	157	N(1D)···N(1B)	$x, y, 1 + z$
8	3.38	3.38	2.67	3.51 [C(8)]	147	N(1)···N(1′)	$-x, -y, -z$
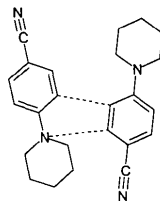
(*c*) π–π type contacts between phenyl and piperidyl nitrogen moieties.

(I) ($n =$)	Distance (Å)	Interplanar Ph···Ph angle (°)	Atoms in contact	Symmetry operation*
7	3.56	17.4	C(5A)···C(5B)	$-x, -y, -z$
	3.54		N(9A)···C(4B)	$-x, -y, -z$
	3.53	12.5	C(7C)···C(5D)	x, y, z
	3.50		N(9C)···C(4D)	x, y, z

* The space-group symmetry operation performed on the second atom to bring it into contact with the first.

(I) ($n = 4$). There are four molecules in the asymmetric unit of the noncentrosymmetric monoclinic space group $P2_1$, giving rise to eight molecules in the unit cell. Crystal packing is illustrated in Fig. 3. Pairs of molecules (*A* and *C*, and *B* and *D*) are stacked in a head-to-tail fashion parallel to *a*. Relative to the ..ACAC.. stack of molecules, the ..BDBD.. stack is displaced by approximately $\frac{1}{4}$ *a* and related by a pseudotwofold screw axis parallel to *a*. The normal distance between phenyl planes is $\frac{1}{2}$ *a* (4.2 Å), but the shortest distance between centroids of phenyl planes is 6.3 Å, which is too long for significant π–π interaction. The closest interchromo-

phoric contact is between a cyano nitrogen of one stack and a phenyl C—H moiety (*meta* to the cyano group) of a neighboring stack alongside but displaced by $\frac{1}{4}$ *a*. Thus, as is apparent in Fig. 3, there is a head-to-tail stepped arrangement linking molecule *A* to *D* to *B* to *C* to *A*..., starting with molecule *A* in the top left-hand corner of the diagram and proceeding stepwise and downwards from left to right. The N_{cyano}···C(7′) distances range from 3.40 to 3.56 Å, a separation similar to the sum of the van der Waals radii for C and N atoms, 1.80 and 1.58 Å, respectively (Kitaigorodsky, 1973). Characteristic interactions between cyanophenyl moieties of neighboring

molecules are summarized in Table 9. Small differences occur. For example, for molecules C and D, the cyano heads also make contact with neighboring piperidyl rings, and the head-to-tail cyano–methyl contacts are ca 0.1 Å shorter than the corresponding contacts of molecules A and B.

(I) ($n = 5$). There are two molecules in the asymmetric unit of the centrosymmetric monoclinic space group $P2_1/c$, giving rise to eight molecules in the unit cell. The crystal packing is illustrated in Fig. 4. As in (I) ($n = 4$), molecules are arranged in antiparallel stacks, ..ABAB.., separated by 4.5 Å, but with a lateral displacement that now has the piperidyl N atoms of adjacent molecules in the stack almost above and below the $ipso$ carbon of the piperidyl substituent of the intervening molecules. Although the environments (and molecular conformations) of the crystallographically independent molecules of (I) ($n = 4$) are remarkably similar, the environments around molecules A and B of (I) ($n = 5$) are dissimilar.

Molecules A form centrosymmetrically related pleated layers parallel to ($\bar{1}01$), where the cyano group is surrounded on either side (and above and below) by alkyl chains (Fig. 4b). Molecules B also form centrosymmetrically related pleated layers, but pairs of cyanophenyl groups are in close side-on contact (Fig. 4c). Although the $N_{cyano} \cdots C(4')$ (carbon $ortho$ to the cyano substituent) contact at 3.52 Å is slightly greater than the sum of the van der Waals radii, the $N_{cyano} \cdots H—C(4')$ separation of 2.60 Å and angle of 161° are consistent with a hydrogen bonding-like interaction (Viswamirta, Radhakrishnan, Bandekar & Desiraju, 1993). Such an interaction has been postulated between the electron-rich cyano N atom and the electron-deficient $ortho$ (to cyano) H atom for benzonitrile dimers in a supersonic jet (Kobayashi, Honna, Kajimoto & Tsuchiya, 1987), although the estimated (and suspiciously short) separation of 2.9 Å between cyano N atoms of the benzonitrile pairs is much shorter than that of 4.4 Å observed for (I) ($n = 5$).
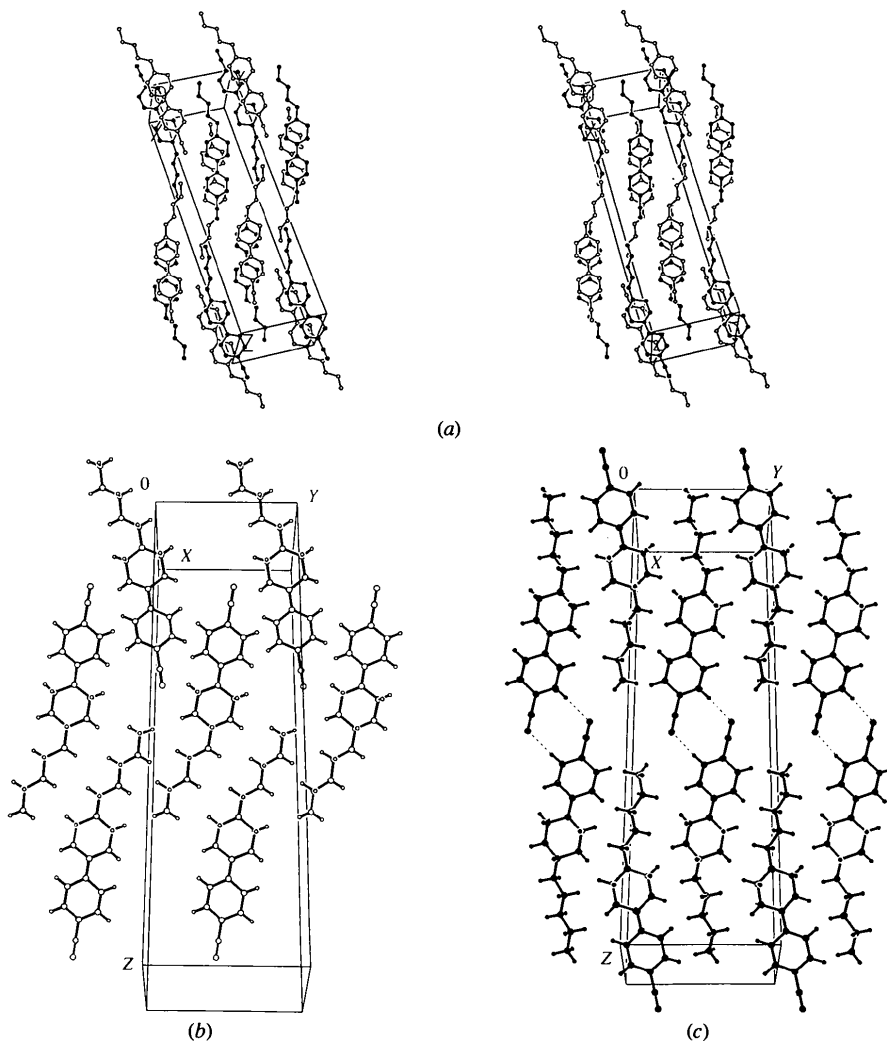

(a)

(b)

(c)

Fig. 4. (a) Stereodiagram of (I) ($n = 5$), viewed approximately down the a axis, showing the stacking of molecules. H atoms are omitted for clarity. Atoms of molecule A are denoted by open circles and atoms of molecules B by filled circles. (b) Diagram showing the packing of molecules A of (I) ($n = 5$) into ruffled layers with pairing of cyanophenyl groups. (c) Diagram showing the packing of molecules B of (I) ($n = 5$) into ruffled interdigitated layers.

Neither the vertical stacking nor the nearly coplanar side-by-side arrangement of molecules leads to significant π–π interactions for (I) ($n = 5$).

(I) ($n = 6$). This homolog has the smallest number of molecules in the unit cell: $Z = 2$ for the centrosymmetric triclinic space group $P\bar{1}$. The antiparallel stacking of molecules that was found for (I) ($n = 4$ and 5) is not seen for (I) ($n = 6$), or for higher homologs (vide supra). A pairwise centrosymmetric interaction of cyanophenyl groups, similar to that of (I) ($n = 5$) is observed, but, in contrast to the antiparallel arrangement of molecules in layers of (I) ($n = 5$), ribbons of adjacent (I) ($n = 6$) molecules are aligned parallel and centrosymmetrically related head-to-head and tail-to-tail (Fig. 5). As a result, in addition to the attractive interaction about one set of inversion centers [$N_{cyano} \cdots (H)C'_{phenyl}$ 3.29 Å], there is a repulsive interaction about the second set of inversion centers ($N_{cyano} \cdots N''_{cyano}$ 3.20 Å). See Table 9 for more details.

(I) ($n = 7$). There are four molecules in the asymmetric unit of the centrosymmetric triclinic space group $P\bar{1}$. Molecules are arranged into two centrosymmetrically related layers parallel to (110), as illustrated in Fig. 6. In a given layer there are two ribbons of antiparallelly arranged molecules, A and D, and C and B. These ribbons are linked by pseudocentrosymmetric interaction

of cyanophenyl groups of molecules A and C [average $N_{cyano} \cdots N'_{cyano}$, 3.51 Å; average $N_{cyano} \cdots C'_{phenyl}$, 3.53 Å; average $N_{cyano} \cdots H(C'_{phenyl})$, 2.66 Å]. In the other layer, a somewhat closer pseudocentrosymmetric interaction of cyanophenyl moieties is found between molecules B and D [average $N_{cyano} \cdots N'_{cyano}$, 3.57 Å; average $N_{cyano} \cdots C'_{phenyl}$, 3.40 Å; average $N_{cyano} \cdots H'(C'_{phenyl})$, 2.51 Å; see also Table 9]. Each layer of molecules in the structure of (I) ($n = 7$) resembles closely the layer of molecules B in (I) ($n = 5$). In contrast to all other homologs, where the closest putative phenyl$\cdots$phenyl π–π contacts exceed 4.2 Å, pairs of phenyl groups of (I) ($n = 7$) molecules are stacked parallel to b, but with a lateral displacement that leaves in close contact only the phenyl C atoms meta to the cyano moiety and the piperidyl N atom and a phenyl C atom ortho to the cyano substituent. Phenyl C atoms are separated by only 3.56 Å for antiparallel molecules A and B, and by 3.53 Å for similarly aligned molecules C and D. The piperidyl nitrogen of molecule A contacts the C atom ortho to the cyano moiety at 3.54 Å for molecules A and B, and at 3.50 Å for molecules C and D. The pairs of phenyl rings are almost coplanar, being tilted by 17.4° for molecules A and B, and 12.5° for molecules C and D. As is apparent in Fig. 6, these contacts correspond to a limited stacking of phenylpiperidyl nitrogen moieties, so that π–π interactions are expected to be weak.

(I) ($n = 8$). There is a single molecule in the asymmetric unit of the centrosymmetric monoclinic space group $P2_1/c$. Molecular packing, illustrated in Fig. 7, possesses elements of the packing of (I) [$n = 4$ and 5 (NB antiparallel stacking of the cyanophenylpiperidyl moieties)] and of (I) [$n = 7$ (NB antiparallel ribbons linked into layers by, in this case, centrosymmetric cyanophenyl interactions)]. However, the cyanophenyl interactions for (I) ($n = 8$) are repulsive ($N_{cyano} \cdots N'_{cyano}$, 3.38 Å; $N_{cyano} \cdots C'_{cyano}$, 3.38 Å; $N_{cyano} \cdots C'_{phenyl}$, 3.51 Å). A second interaction, reminiscent of that in (I) ($n = 4$), is found between the cyano N atom and a C atom meta to the cyano substituent of a glide-plane related molecule. Within layers, the molecules are extensively interdigitated.
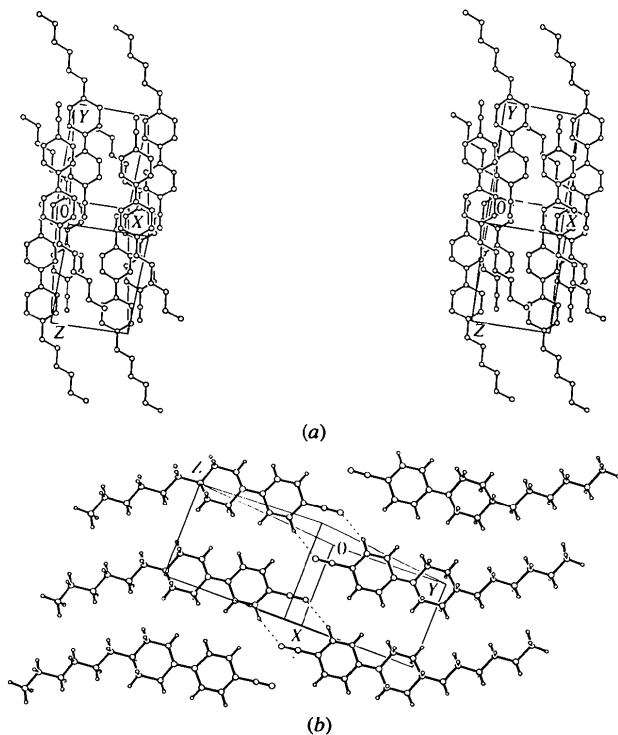

(a)

(b)

Fig. 5. (a) Stereodiagram of (I) ($n = 6$), viewed approximately onto the (011) plane, showing the relative disposition of layers. H atoms are omitted for clarity. (b) Diagram showing the parallel alignment of molecules into ribbons and the centrosymmetric stitching together of ribbons to give a layer of (I) ($n = 6$).

Discussion

For molecular crystals of (I) ($n = 6$ and 7), both in space group $P\bar{1}$, there is a centrosymmetric partner for each molecule. As a result, zero bulk polarization is expected. The noncentrosymmetric $P2_1$ space group of (I) ($n = 4$) crystals contains a twofold screw axis perpendicular to the molecular orientation. Thus, the bulk polarization should be zero as in the centrosymmetric $P\bar{1}$ unit cell. The $P2_1/c$ space group of (I) ($n = 5$) also has its twofold screw axis perpendicular to the molecular orientation, in addition to the center of symmetry. This, again, yields a predicted zero polarization.

Large dipole moments had been thought to be an important factor in obtaining organic crystals with molecular packing conforming to one of the centrosymmetric space groups (for example $P\bar{1}$; Nicoud & Twieg, 1987). Recently, Whitesell, Davis, Saunders, Wilson & Feagens (1991) carried out a statistical analysis of the molecular dipole moments of organic crystals within the space groups $P1$, $P\bar{1}$ and $P2_1$, and found that the magnitude of the dipole moments does not correlate with the relative molecular orientations.

Gavezzoti (1990) compared the relative orientation of cyano and carbonyl groups in organic crystals and found that parallel stacking of dipoles is not favored, except when attractive van der Waals forces dominate the packing, as in the case of 9-cyanoanthracene (Rabaud & Clastre, 1959). Antiparallel stacking of the dipoles is the most common structural motif, resulting in centrosymmetric unit cells. In such cases, approach of atoms in

dipolar groups is as short as the sum of their van der Waals radii [NB I ($n = 6$ and 7)]. However, when the distance between dipole centroids of neighboring molecules exceeds ca 5 Å, the relative orientations of the dipoles are not restricted to being antiparallel and can assume a wide range of angles which are determined by steric and other packing factors. This may be a factor in establishing a noncentrosymmetric unit cell in (I) ($n = 4$). The presence of both centrosymmetric ($P\bar{1}$ and $P2_1/c$) and noncentrosymmetric ($P2_1$) unit cells of the (I) series indicates that dipole–dipole interactions, while important, do not completely control the packing arrangements of their crystals. The differences in packing arrangements may be related to the ability of the longer alkyl chains, (I) ($n = 7$ and 8), to fill lattice spaces near the bulky N-phenylpiperidyl group better than the shorter butyl, pentyl or hexyl chains. An extended heptyl or octyl chain is almost long enough to span the long axis of
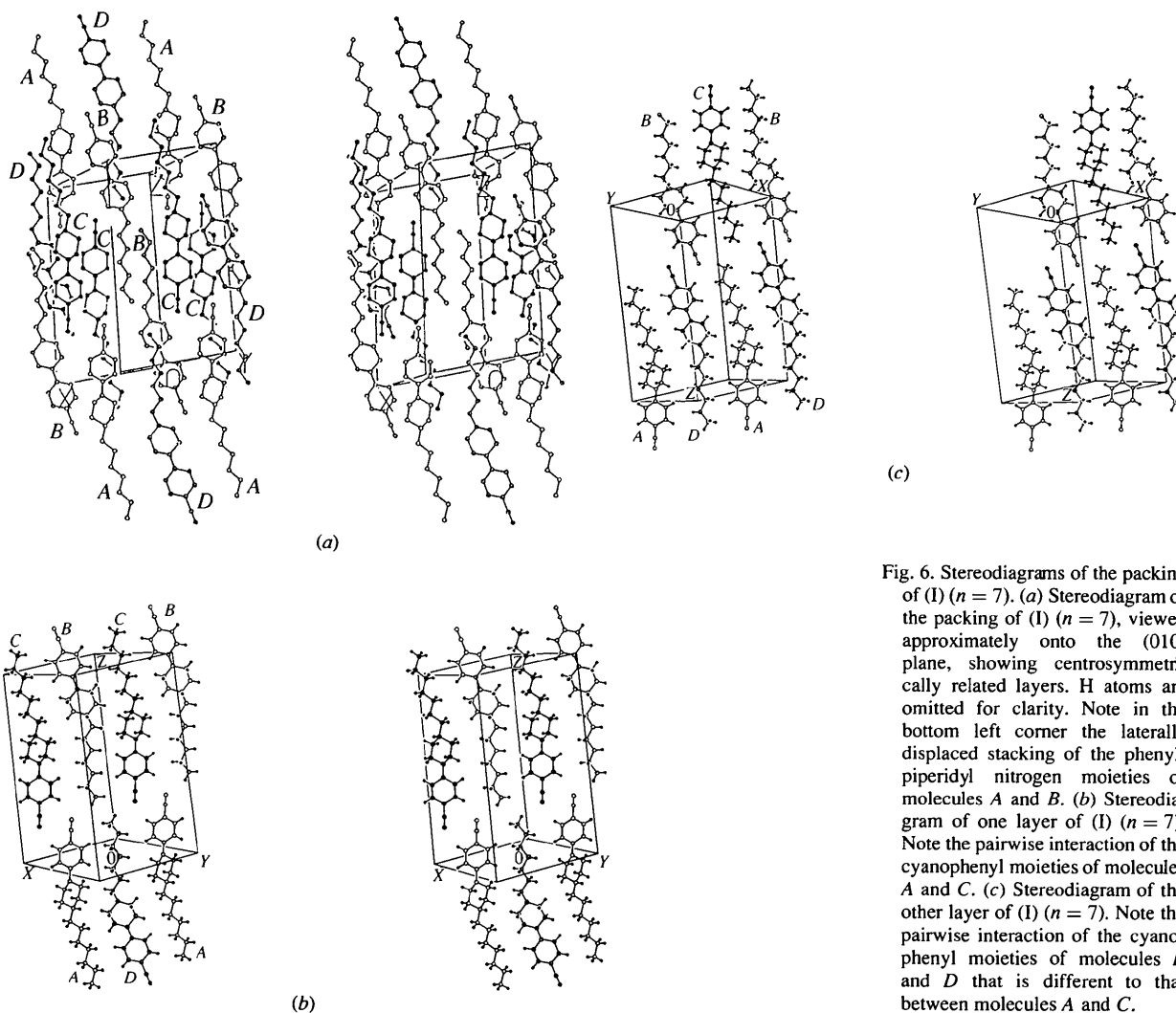

(a)

(b)

(c)

Fig. 6. Stereodiagrams of the packing of (I) ($n = 7$). (a) Stereodiagram of the packing of (I) ($n = 7$), viewed approximately onto the (010) plane, showing centrosymmetrically related layers. H atoms are omitted for clarity. Note in the bottom left corner the laterally displaced stacking of the phenylpiperidyl nitrogen moieties of molecules A and B. (b) Stereodiagram of one layer of (I) ($n = 7$). Note the pairwise interaction of the cyanophenyl moieties of molecules A and C. (c) Stereodiagram of the other layer of (I) ($n = 7$). Note the pairwise interaction of the cyanophenyl moieties of molecules B and D that is different to that between molecules A and C.

the phenylpiperidyl rings; the butyl, pentyl or hexyl chains are not. Although the electronic absorption and emission characteristics of (I) ($n = 6, 7$ and 8) are similar to each other and distinctly different from those of (I) ($n = 4$ and 5; Sheikh-Ali, Rapta, Jameson, Cui & Weiss, 1994), the molecular packing of (I) ($n = 6$), where ribbons of molecules are aligned parallel, is not the same as those of the heptyl or octyl homolog, where ribbons of molecules are aligned antiparallel. In any event, the arrangement of molecules into flat layers [I ($n = 6, 7$ and 8)], stepped layers and stacks [I ($n = 5$) and I ($n = 4$)] does appear to correlate with the different electronic absorption and emission characteristics of these molecules in the crystalline state. It is not clear whether the molecular packing will continue to change as the length of the alkyl chain is further increased.

Other considerations

The relationship between molecular organization in the solid phase and the occurrence and the type of mesophase derived therefrom has been reviewed by
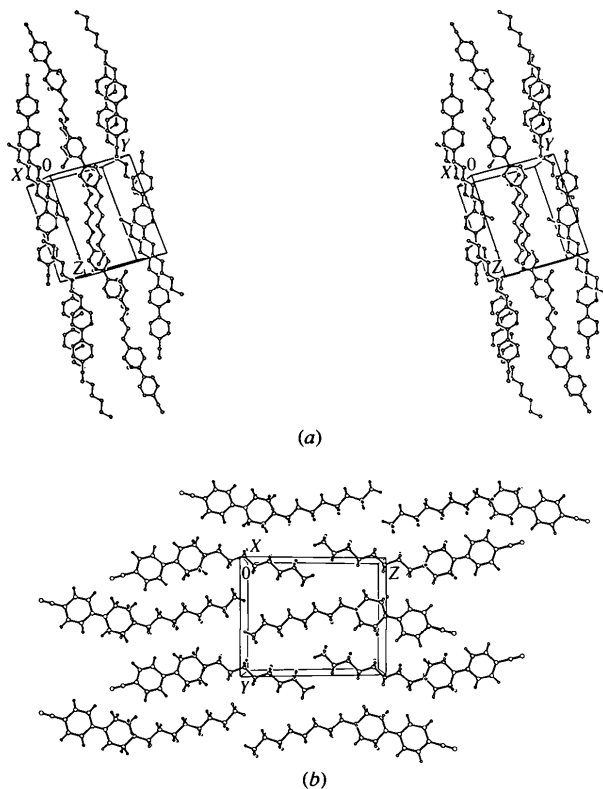

(a)

(b)

Fig. 7. (a) Stereodiagram of the packing of (I) ($n = 8$), viewed approximately down the a axis, showing the stacking of molecules and the centrosymmetric, pairwise interaction of cyanophenyl moieties. H atoms are omitted for clarity, and disordered piperidyl atoms are shown as closed circles. (b) Diagram showing the interdigitated packing of molecules in a layer.

Bryan (1982). Molecular parallelism in the crystalline phase was found to be common among nematogens. The general consensus is that a spontaneous decrease in the molecular order occurs during the transition to the fluid state, and a residual orientational ordering is retained only if molecular parallelism exists prior to melting. While the parallel imbrication of molecules is a necessary condition for a solid to yield a mesophase, failure of certain crystals with such arrangements (e.g. p-hydroxycinnamic acid; Bryan, 1982) to yield mesophases indicates that it is not sufficient. This appears to be the case for the molecules of (I) which have their directors almost parallel to each other, but do not yield a mesophase upon melting (Sheikh-Ali & Weiss, 1991). The crystal structure of (I) ($n = 6$) shows the highest degree of molecular parallelism of all the homologs. Apparently, melting occurs at temperatures where significant rotational motion about all three axes is permitted and, thus, the crystal cannot yield a mesophase. However, a monotropic nematic phase can be obtained by supercooling either (I) ($n = 6$; Karamysheva et al., 1981) or a binary mixture of any pair of homologs (Sheikh-Ali & Weiss, 1991).

Since molecules of (II) generally do form mesophases while those of (I) generally do not, it is interesting to note how they differ in their crystalline conformations. The most important glaring difference seems to be in the angle of twist between the aromatic and nonaromatic rings: whereas overlap of the lone pair of electrons of the amino N atom and the π-system of the phenyl ring allows the rings of (I) to be almost untwisted, the ipso-C—H of the cyclohexyl ring of (II) cannot have a similar overlap and the phenylcyclohexyl ring system adopts a very twisted conformation. As a result, the alkyl chains of (I) and (II) are projected along very different axes with respect to the aromatic planes. The extended C chains of (I) can be included in a rough plane which makes a relatively small acute angle with the plane described by the phenyl ring (Table 8); the plane of the extended chain of (II) is almost orthogonal to that of the phenyl ring.

An even more interesting aspect of this work is the enormous effect that a methylene unit has on molecular packing. From Table 1, the volume occupied by each molecule of (I) in a unit cell is 363 ($n = 4$), 386 ($n = 5$), 404 ($n = 6$), 429 ($n = 7$) and 464 Å^3 ($n = 8$). None of the increments, except for that between $n = 7$ and 8, are near the 34 Å^3 calculated to be the van der Waals volume of a —CH$_2$— group (Bondi, 1964). This indicates that the (I) homologs pack in a progressively more efficient manner as the alkyl chain length increases at least up to $n = 7$. Since the overall shape of the molecules remains roughly cylindrical, the abrupt change in the crystal space groups must result from variations in the molecular aspect ratios and in the balance between dipolar and dispersive interactions. Presumably, with sufficiently long chains, molecular packing would be lamellar, like that observed for long n-alkanes, n-alkanones and n-alkyl

esters (Broadhurst, 1962). In fact, many molecules may suffer analogous changes in their crystal packing arrangements as an appended alkyl group is lengthened or shortened. It should be possible to catalog and exploit these changes in designing materials for specific uses (*e.g.* Nicoud & Twieg, 1987).

References

BONDI, A. (1964). *J. Phys. Chem.* **68**, 441–451.
BROADHURST, M. G. (1962). *J. Res. Natl. Bur. Stand. Sect. A*, **66**, 241–249.
BRYAN, R. F. (1982). *Zh. Struk. Khim.* **23**, 128–147.
EIDENSCHINK, R., ERDMAN, D., KRAUSE, J. & POHL, L. (1977). *Angew. Chem. Int. Ed. Engl.* **16**, 100.
FURMANOVA, N. G. & TIMOFEEVA, T. V. (1986). *Sov. Phys. Crystallogr.* **31**, 601–603.
GAVEZZOTI, A. (1990). *J. Phys. Chem.* **94**, 4319–4325.

JAMESON, G. B., SHEIKH-ALI, B. M. & WEISS, R. G. (1994). *Acta Cryst.* B50, 703–707.
KARAMYSHEVA, L. A., KOVSHEV, E. I., PAULUCHENKO, A. I., ROITMAN, K. V., TITOV, V. V., TORGOVA, S. I. & GREBENKIN, M. F. (1981). *Mol. Cryst. Liq. Cryst.* **67**, 241–251.
KITAIGORODSKY, A. I. (1973). *Molecular Crystals and Molecules.* New York: Academic Press.
KOBAYASHI, T., HONMA, K., KAJIMOTO, O. & TSUCHIYA, S. (1987). *J. Chem. Phys.* **86**, 1111–1117.
LOWRY, T. M. & RICHARDSON, K. S. (1987). *Mechanism and Theory in Organic Chemistry*, p. 154. New York: Harper & Row.
NICOUD, J. F. & TWIEG, R. J. (1987). *Non-Linear Optical Properties of Organic Molecules and Crystals*, edited by D. CHEMLA & J. ZYSS, Vol. 1, p. 253. New York: Academic Press.
PAULUS, H. & HAASE, W. (1983). *Mol. Cryst. Liq. Cryst.* **92**, 237–242.
RABAUD, H. & CLASTRE, J. (1959). *Acta Cryst.* **12**, 911–915.
SHEIKH-ALI, B. M. & WEISS, R. G. (1991). *Liq. Cryst.* **10**, 575–580.
SHEIKH-ALI, B. M. & WEISS, R. G. (1994). *Liq. Cryst.* **17**, 605–615.
SHEIKH-ALI, B. M., RAPTA, M., JAMESON, G. B., CUI, C. & WEISS, R. G. (1994). *J. Phys. Chem.* **98**, 10412–10418.
SHELDRICK, G. M. (1985). *SHELXS86. Program for the Solution of Crystal Structures.* Univ. of Göttingen, Germany.
SHELDRICK, G. M. (1995). *J. Appl. Cryst.* In preparation.
VISWAMIRTA, M. A., RADHAKRISHNAN, R., BANDEKAR, J. & DESIRAJU, G. R. (1993). *J. Am. Chem. Soc.* **115**, 4868–4869.
WHITESELL, J. L., DAVIS, R. E., SAUNDERS, L. L., WILSON, R. J. & FEAGENS, J. P. (1991). *J. Am. Chem. Soc.* **113**, 3267–3270.

Acta Cryst. (1995). B51, 835–838

Electrostatic Potentials from Charge-Density Studies of Benzamide at 123 K

BY J. R. RUBLE

Department of Crystallography, University of Pittsburgh, Pittsburgh, PA 15260, USA

AND A. GALVAO

Centro de Tecnologia Quimica e Biologica, 2780 Oeiras, Portugal

Abstract

C_7H_7NO, $M_r = 121.14$, monoclinic, $P2_1/c$, $a = 5.549$ (1), $b = 5.033$ (1), $c = 21.548$ (4) Å, $\beta = 89.22$ (1)°, $V = 601.74$ (1) Å^3, $D_x = 1.35$ Mg m^{-3}, $\lambda(Mo K\alpha) = 0.71069$ Å, $\mu = 0.086$ mm^{-1}, $F(000) = 256$, $T = 123$ K, final $R = 0.049$, $wR = 0.047$, $S = 1.457$ for 3527 reflections and 213 parameters, including multipole electron-population parameters up to octapole for non-H atoms and quadrapole for H atoms.

Introduction

A charge-density study of benzamide was undertaken as part of a study of the charge density of benzene and its derivatives obtained by experimental methods and theoretical calculations (Jeffrey, Ruble, McMullan & Pople, 1987; Stewart, 1991). Electrophilic aromatic

substitution has been examined by a number of different researchers. March (1992), Carey & Sundberg (1990) and Taylor (1990) agree that first the rapid formation of a π-complex occurs, followed by the slower formation of a σ-complex in which one C atom has a H plus the electrophile, followed finally by the rapid loss of either the H or the electrophile. The orientational effects observed in monosubstituted aromatic compounds are caused by stabilization of one σ-complex and destabilization of the other. Pauling (1960) points out that the distribution of charge in the molecule undergoing substitution is an important consideration in determining the orientation of the next substituent. Since the substituent in benzamide is a *meta*-director for further electrophilic addition, there was a question as to whether this effect would be observed in the electrostatic potential, or whether it would be masked by intermolecular interactions. Results of the present study are